# Supporting information

## Targeting liposome and accelerated CRISPR system for selective imaging miR-21 in cell

Wenyue Zhang[1], Mengting Wu[1], Qingqing Zhang[1], Xibin Chen[2], Yingshu Guo[1]*

[1]School of Chemistry and Chemical Engineering, Qilu University of Technology (Shandong Academy of Sciences), Jinan 250353, China

[2]Shandong GuoChen Biotechnology Co., Ltd., Jinan 250353, China

E-mail: yingshug@126.com

## 1. Materials and Equipments

### 1.1 Materials and reagents

All oligonucleotides (Table S1) were obtained by Shanghai Sangon Biological Engineering Technology & Services Co., Ltd. (Shanghai, China). Lba Cas12a(Cpf 1)、2.1 NE Buffer (1×) (50 mM NaCl，10 mM Tris-HCl, 10 mM $MgCl_2$, 100 μg/ml Recombinant Albumin, pH=7.9) were purchased from New England Biolabs (Beijing, China). 1,2-distearoyl-sn-glycero-3-phosphoethanolamine-N-(methoxy(poly (ethylene glycol)) $_{2000}$) (DSPE-$PEG_{2000}$) was purchased from Guangzhou Weihua Biotechnology Co., Ltd.. 1,2-distearoyl-sn-glycero-3-phosphocholine (DSPC) and cholesterol (Avanti lipids) were purchased from Macklin Inc. Cell culture plates were purchased from NEST Biotechnology Co. Ltd. (China). Calcein/PI cell viability/cytotoxicity assay kit, methyl thiazolyl tetrazolium (MTT), DAPI were purchased from Beyotime Biotechnology (Shanghai, China). Dulbeccos modified eagles medium (DMEM), antibiotics (penicillin-streptomycin, PS), trypsin (0.25% EDTA), cell lysis buffer for western and IP without inhibitors were purchased from Solarbio. Fetal bovine serum (FBS) were purchased from Gibco Life Technologies. Ethanol were obtained from Sinopharm Chemical Reagent Co., Ltd.. MCF-7 cells were provided by Procell Life Technology (Wuhan, China).

### 1.2 Equipments

The morphology of the nanoparticles was photographed using transmission electron microscopy (TEM, JEOL JEM2100). Size and zeta potential data were collected with a Malvern Zetasizer Nano ZS90. Ultraviolet–visible absorption spectra (UV/vis) were measured by an Agilent Cary 60 UV-vis Spectrophotometer. The Hitachi FL-4700 was used to detect and record the fluorescence signals. The Nikon Ti2-E microscope was utilized to acquire the fluorescence images. Fluorescence imaging was evaluated by High Content Imaging System (PerkinElmer Opera Phenix). Flow cytometry measurements were performed on Beckman Coulter, CytoFLEX. Agarose gel electrophoresis was imaged using an automated gel imaging analysis system (Shanhai Peiqing Science & Technology Co., Ltd, JS-2012).

## 2. Experimental procedures

### 2.1 The preparation of $MnO_2$ NS.

12 mL of 3,3'5,5’-tetramethyl benzidine dihydrochloride (TMA) solution (0.1 M) with 2 mL of

$H_2O_2$ (30 wt.%) and 6 mL of ultrapure water were mixed to Solution A. Solution B was made by dissolving $MnCl_2 \cdot 4H_2O$ (0.6 g) in 10 mL of water. Solution A was then rapidly mixed with Solution B within 15 seconds. The mixture turned deep brown, indicating that $Mn^{2+}$ had been oxidized to $Mn^{4+}$. The resulting deep brown suspension was vigorously stirred at room temperature overnight to obtain bulk $MnO_2$. The prepared bulk $MnO_2$ was centrifuged at 2000 rpm for 10 minutes and washed three times with distilled water and methanol. Afterward, the bulk $MnO_2$ was dried at 60°C and stored for later use. To prepare the $MnO_2$ NS, 10 mg of the bulk $MnO_2$ was dispersed in 20 mL of water and subjected to ultrasonic treatment for 10 h.[1]

**2.2 The preparation of $MnO_2$/Cas12a/crRNA/FQDNA**

$MnO_2$/Cas12a/crRNA/FQDNA was prepared by mixing 100 μL of $MnO_2$ NS (100 μg/mL), 3 μL of crRNA (50 μM) and 3 μL of FQDNA (50 μM) for 20 min, followed by addition of 10 μL of Tris-HAc buffer (100 mM, pH 7.4). After that, 8 μL Cas12a (10 μM) was added into above mixture and incubated for another 20 min at room temperature to obtain $MnO_2$/Cas12a/crRNA/FQDNA.

**2.3 The preparation of Lip@substrate.**

Three different lipids of designated molar ratios were used in the synthesis of liposomes: 1,2-distearoyl-sn-glycero-3-phosphocholine (DSPC), 1,2-distearoyl-sn- glycero-3-phosphoethanolamine-N-(polyethylene glycol) (DSPE-$PEG_{2000}$), and cholesterol (Avanti lipids). (2:0.1:1) Briefly, a lipid mixture (2.25 μmol in total) in chloroform was added to a round-bottom flask, blown dry with purified argon, and desiccated by vacuum to form a thin film at the bottom of the flask. For formation of empty liposomes, 300 μL of PBS buffer was added to hydrate the lipid film through vortex and short bursts of sonication in a water bath. After hydration, the lipid film resuspension was extruded using polycarbonate membrane with a pore size of 100 nm 19 times at 70 °C. The resulting liposomes were then stored at 4°C for all experiments. For encapsulation of nucleic acid molecules inside the liposomes, a DNA oligo of substrate was dissolved in PBS buffer at a concentration of 100 nM, and 300 μL of this solution was used to hydrate the lipid film as described above, followed by extrusion using polycarbonate membrane with a pore size of 100 nm 35 times at 70°C. [2]

**2.4 The preparation of Lip@substrate/Apt.**

After dispersing the previously synthesized Lip@substrate (100 μL) in MUC1 aptamer aqueous solution (1 OD), it underwent a one-minute ultrasonography treatment. For a full day in the dark, the solution was slowly stirred. After that, the unbound aptamert was removed from the Lip@substrate/Apt by centrifuging and repeatedly washing. Finally, Lip@substrate/Apt was dispersed in the PBS solution.

**2.5 Feasibility analysis of $MnO_2$/Cas12a/crRNA/FQDNA combined with substrate in solution.**

2.5 μg/mL $MnO_2$ NS was incubated with 0.5 mM GSH. 2 min latter, 2.1 NE Buffer (1×), substrate (100 nM), Cas12a (50 nM), crRNA (100 nM), FQDNA (100 nM), and differenct concentrations of miR-21 were added to a total volume of 100 μL. The mixture was incubated at 37ºC for 10 min. The fluorescence spectrum was recorded with an excitation wavelength of 488 nm.

**2.6 Agarose gel electrophoresis analysis**

Nucleic acid reaction samples were subjected to 2% agarose gel electrophoresis at a fixed potential of 120 V, using 1 × TAE buffer as the electrophoretic buffer. In the pretreatment stage, the ratio of nucleic acid solution to sample buffer was 5:1 (V/V). After electrophoresis, image was captured using the gel imaging analysis system.

**2.7 Cell culture**

MCF-7 cells were cultured in DMEM medium containing 1% penicillin-streptomycin and 10% fetal calf serum. These cell lines were maintained in a 5% $CO_2$ atmosphere at 37℃

**2.8 MTT test**

MCF-7 cells were inoculated into 96-well plates with a cell density of $1\times10^6$ cells per well and then treated with different samples of different concentrations for 48 h. After removing the supernatant, 100 μL fresh medium (containing 10% MTT solution) was added, and continued to culture for 4 h. The supernatant was removed and 100 μL DMSO was added to each micropore. Then 96-well plate was shaken at a low speed for 10 min to completely dissolve the crystals. Finally, the absorbance of each hole was measured using a microplate reader.

**2.9 The analysis of $MnO_2$/Cas12a/crRNA/FQDNA+Lip@substrate/Apt targeting MCF-7 cell**

MCF-7 cells were inoculated into a 12-well plate with a cell density of $1 \times 10^6$ cells per well and washed three times with PBS buffer. 50 μL Lip@substrate/Apt was incubated with MCF-7 cells for 2 h. The cells were washed three times with PBS buffer. 500 μL of fresh cell growth medium supplemented with $MnO_2$/Cas12a/crRNA/FQDNA was added for 0, 0.5, 1, 2 h. The cells were washed three times with PBS buffer, stained with DAPI for 15 min, and subjected to fluorescence microscope imaging and flow cytometry counting.

**2.10 High-content fluorescence imaging**

Lip@substrate/Apt (10 μL) was incubated with MCF-7 cells for 2 h in 96-well plates. The cells were washed three times with PBS buffer. 100 μL of fresh cell growth medium containing $MnO_2$/Cas12a/crRNA/FQDNA was added. After 2 h, the cells were washed three times with PBS buffer and stained with DAPI for 15 min. High-content fluorescence imaging was performed.

**3. Supplementary figures**

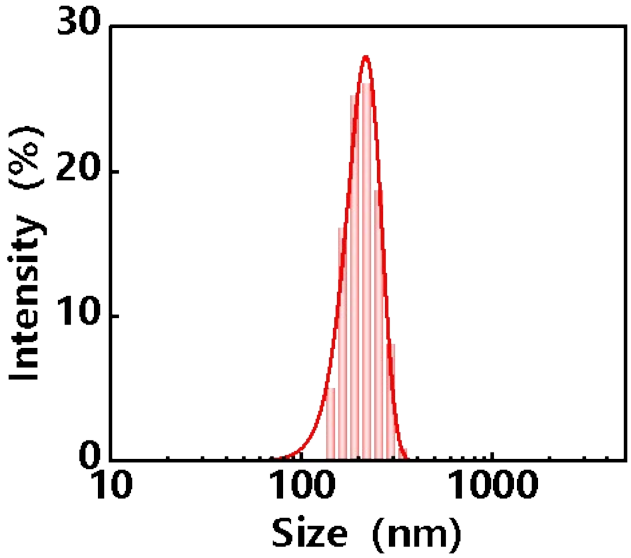


**Fig. S1.** Hydrodynamic diameters of $MnO_2$/Cas12a/crRNA/FQDNA by DLS.

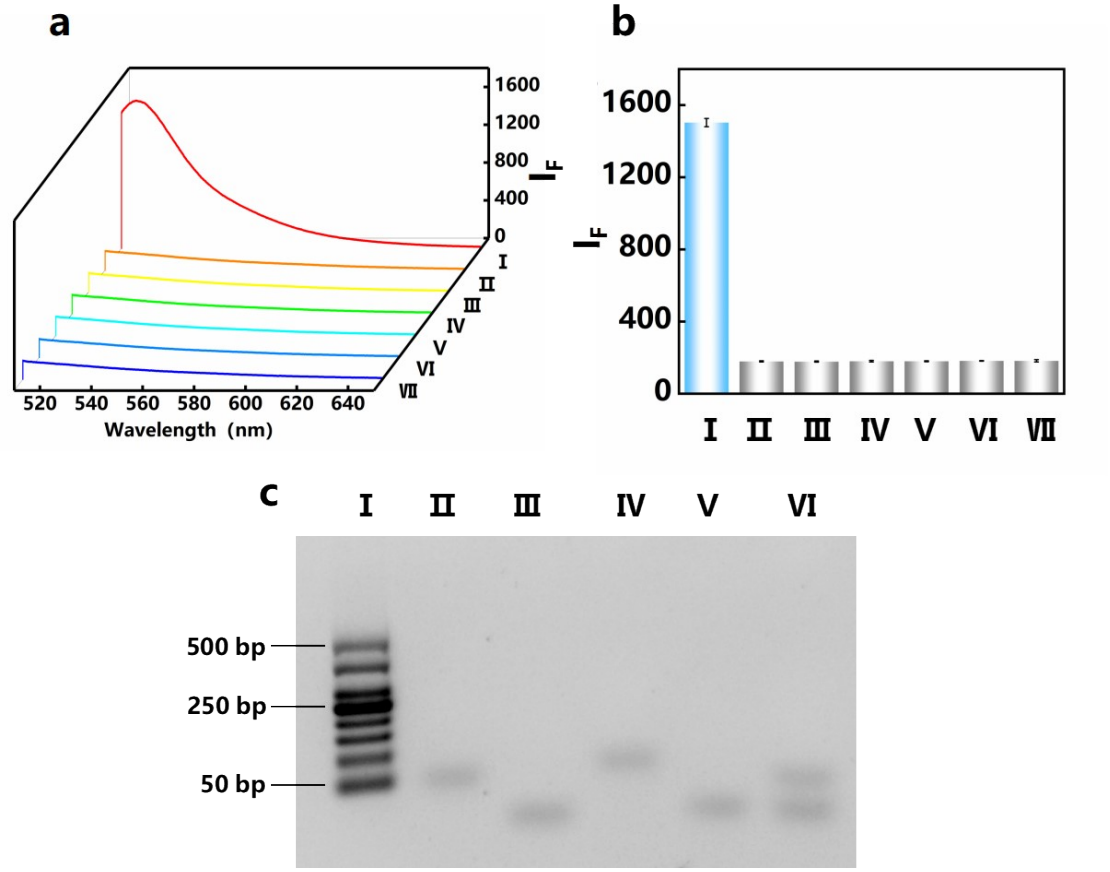


**Fig. S2**. (a) Fluorescence spectrogram of the specific response of miR-21. (I: miR-21；II: Blank；III: miR-10b；IV: miR-141；V: miR-let-7f；VI : miR-210；VII: miR-let-7a) (b) Fluorescence intensity of MCF-7 cells vs (a). (c) Agarose gel electrophoresis imaging. (I: marker；II: substrate； III: miR-21；IV: substrate+miR-21；V: miR-10b；VI : substrate+miR-10b)

Fig. 2a shown the operating mechanism of the sensor system based on CRISPR. The double-stranded nucleic acid formed by the complementary pairing of the purple sequence in the substrate and the purple sequence of crRNA became the key substance for activating the trans-cleavage performance of the CRISPR/Cas12a system. To regulate this activation function, we designed a blue nucleic acid sequence in the substrate to complement the purple sequence in the substrate, in order to shut down the trans-cleavage performance of the CRISPR/Cas12a system. If the number of complementary pairs between the purple nucleic acid sequence in crRNA and the purple sequence in the substrate was too large, the trans-cleavage activity could not be completely shut

down. This was due to the high stability and strong competitiveness of the double strands. One feasible way to solve this problem was to reduce the number of complementary pairs between the purple sequences in crRNA and those in the substrate. However, reducing complementary base pairs by simply shortening or inserting mismatched bases inevitably resulted in a great loss of trans-cleavage activity. It was ideal to reduce complementary base pairs while maintaining high trans-cleavage activity. The "RESET" effect found by Kong et al. perfectly resolved this contradiction. [3-6] The 13+3 activator (purple sequence) contained a total of 16 base sequences complementary to the crRNA, and the complementary base sequence could be split into 13 and 3-base parts by inserting a single mismatching base (T). Because of the weak stability of the crRNA/13+3 duplex, 13+3 was unable to activate trans-cleavage activity. However by adding a hairpin-like crRNA-independent sequence to the 3' end of 13+3 (yellow sequence), the acquisition of 13+3R (purple sequence + yellow sequence) activated trans-cleavage activity due to the "hairpin" effect. Interestingly, the 13+3R-activated trans-cleavage activity could be effectively turned off by the addition of a blue sequence partially complementary to 13+3R. Thus, a low background could be ensured, which enabled the design of "on-off-on" biosensors. In the design of this paper, the purple sequence in the substrate must be complementary to crRNA under specific conditions to activate the trans-cleavage performance of the CRISPR/Cas12a system. This specific condition refereed to the existence of miRNA-21.

When miR-21 was replaced with other RNAs, the sensing system also did not produce fluorescence, demonstrating the specific response of this approach to miR-21 (Fig. S2a and b, ESI†). In order to further verify the specific recognition of substrate and miR-21, miR-10b was used as a control. Through agarose gel electrophoresis imaging analysis, it could be clearly seen that miR-21 and miR-10b passed through the gel pores rapidly, and the molecular weight of substrate was larger than that of miR-21 and miR-10b, shuttling slower in the gel pores. When the substrate was bound to miR-21, the molecular weight was further increased and the shuttle speed was slower. However, the group of substrate and miR-10b showed two bands, which coincided with the separate substrate and miR-10b, respectively. Therefore, the substrate could specifically recognize miR-21 (Fig. S2c, ESI†).

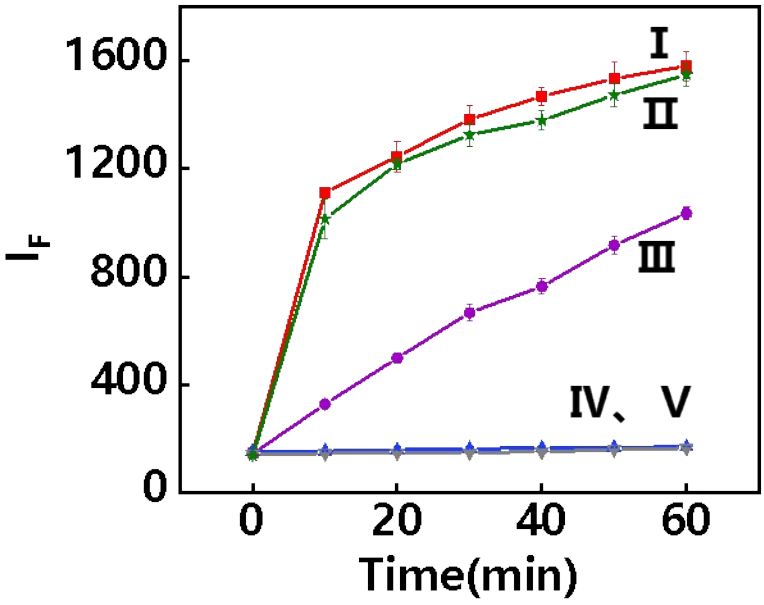


**Fig. S3**. Fluorescence time plots given by different systems. (I: miR-21+GSH+substrate +$MnO_2$/Cas12a/crRNA/FQDNA; II: miR-21+substrate+$Mn^{2+}$+Cas12a/crRNA/FQDNA; III: miR-21+substrate+Cas12a/crRNA/FQDNA; IV: miR-21+substrate+$MnO_2$/Cas12a/crRNA/FQDNA; V: GSH+substrate+$MnO_2$/Cas12a/crRNA/FQDNA)

By monitoring the fluorescence over time under different conditions, we found that the fluorescence response of free CRISPR/Cas12a to miR-21 was slow, and the fluorescence growth lasted for 60 min. In contrast, the fluorescence enhancement of the GSH-assisted $MnO_2$ NS was greatly accelerated, reaching a high fluorescence intensity within 10 min of the reaction. This was comparable to the results of control experiments in which $Mn^{2+}$ was added. These results suggested that the binding of $MnO_2$ NS to GSH could play an accelerating role, enabling the rapid analysis of miR-21.

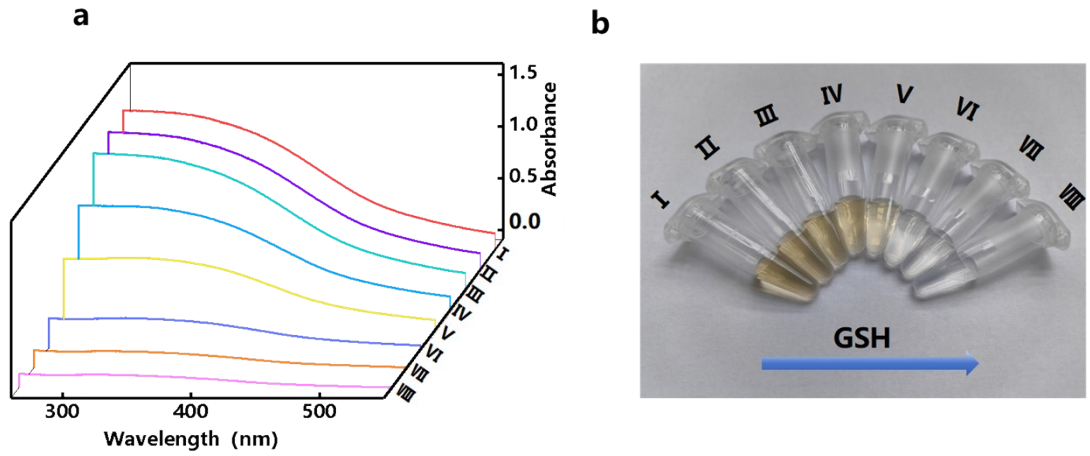


**Fig. S4**. (a) UV/vis spectra of $MnO_2$ NS+GSH. (I-VIII: 0, 0.01, 0.02, 0.05, 0.1, 0.2, 0.5, 1 mM GSH). (b)The corresponding picture of (a).

Since the conversion of $MnO_2$ to $Mn^{2+}$ was a key step, this paper studied the decomposition behavior of $MnO_2$ NS induced by glutathione. As shown, after coincubation of $MnO_2$ NS with different concentrations of GSH, the characteristic absorption band of $MnO_2$ NS at 380 nm almost disappeared, indicating that the $MnO_2$ NS was completely destroyed by GSH. Considering that the concentration of GSH in cancer cells is about 1-10 mM, it could be ensured that the $MnO_2$ NS were completely decomposed within cells, thereby achieving the release of the CRISPR/Cas12a system.

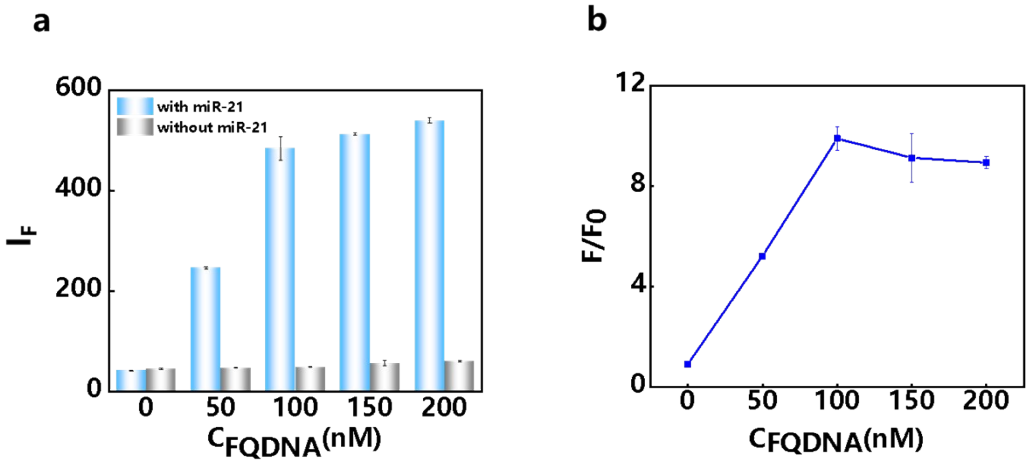


**Fig. S5**. (a) Fluorescence intensity in the presence or absence of miR-21 at different FQDNA concentrations. (b) Ratio of fluorescence signals of different FQDNA concentration.

Before applying $MnO_2$/Cas12a/crRNA/FQDNA to live cells, we first tested their ability to sense miR-21 in solution. To obtain the optimal signal output, we optimized the experimental concentration of FQDNA. The signal output was found to be strongest at 100 nM FQDNA.

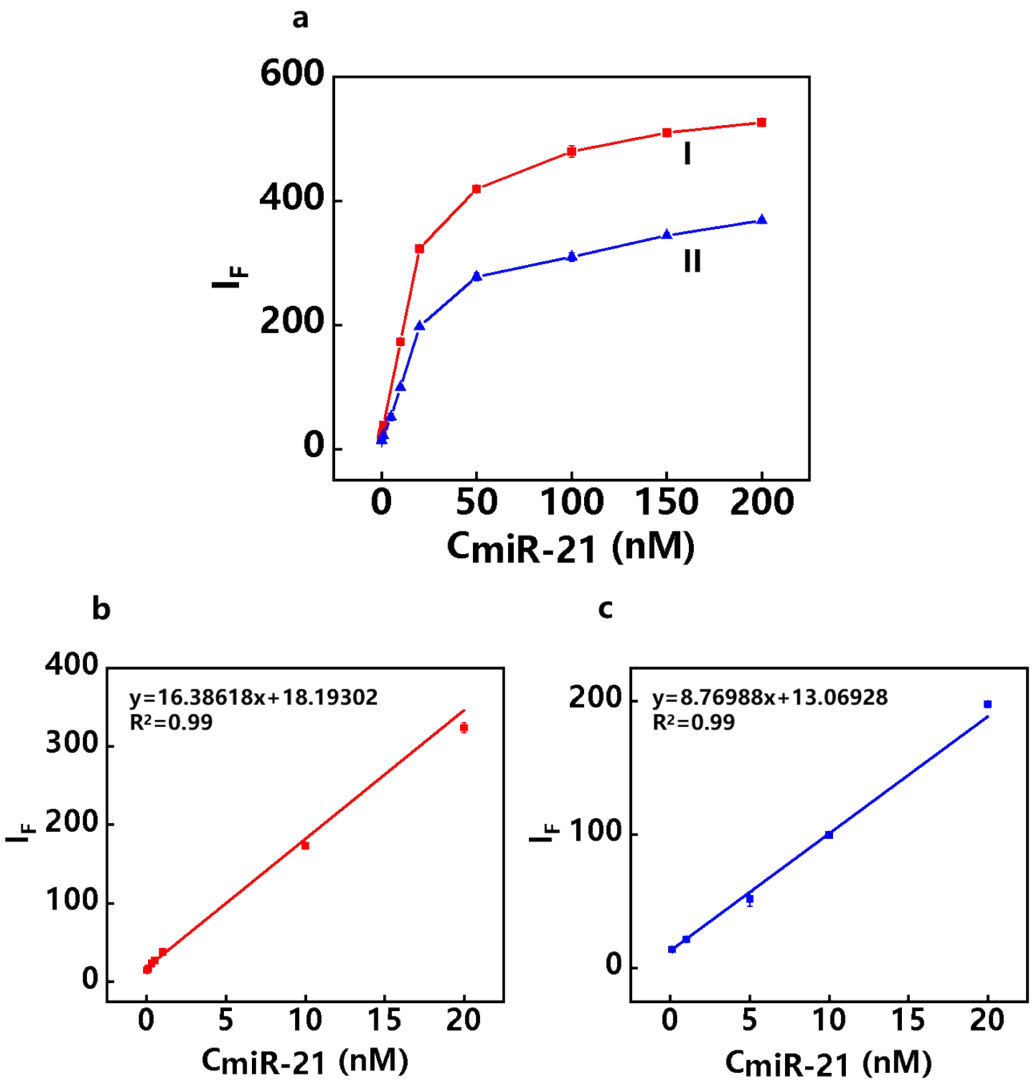


**Fig. S6**. (a) The fluorescence intensity of different systems responding to different concentrations of miR-21. (I: $MnO_2$/Cas12a/crRNA/FQDNA/substrate+GSH; II: Cas12a/crRNA/FQDNA/substrate+GSH). Linear relationships under different systems with miR-21 at different concentrations. (b) $MnO_2$/Cas12a/crRNA/FQDNA/substrate+GSH (miR-21: 0.01、0.1、0.3、0.5、1、10、20、50、100、150、200 nM) (c) Cas12a/crRNA/FQDNA/substrate+GSH (miR-21: 0.1、1、5、10、20、50、100、150、200 nM)

Through the fluorescence signals of different concentrations of miR-21 under different sensing systems (Fig. S6a), it was found that the fluorescence signals of the $MnO_2$/Cas12a/crRNA/FQDNA group were more intense, showing a good linear relationship in the concentration range of miR-21 from 0.01 to 20 nM (Fig. S6b). To highlight the contribution of

$Mn^{2+}$ produced by GSH-induced disassembly of $MnO_2$ NS, we investigated the miR-21 sensing performance of the free CRISPR/Cas12a for comparison. As mentioned above, the fluorescence response of CRISPR/Cas12a to miR-21 in the absence of $Mn^{2+}$ assistance was much slower, and the fluorescence signal output was significantly reduced, with a linear relationship in the concentration range of miR-21 from 0.1 to 20 nM (Fig. S6c). Taken together, $MnO_2$/Cas12a/crRNA/FQDNA/substrate provided good assay sensitivity.

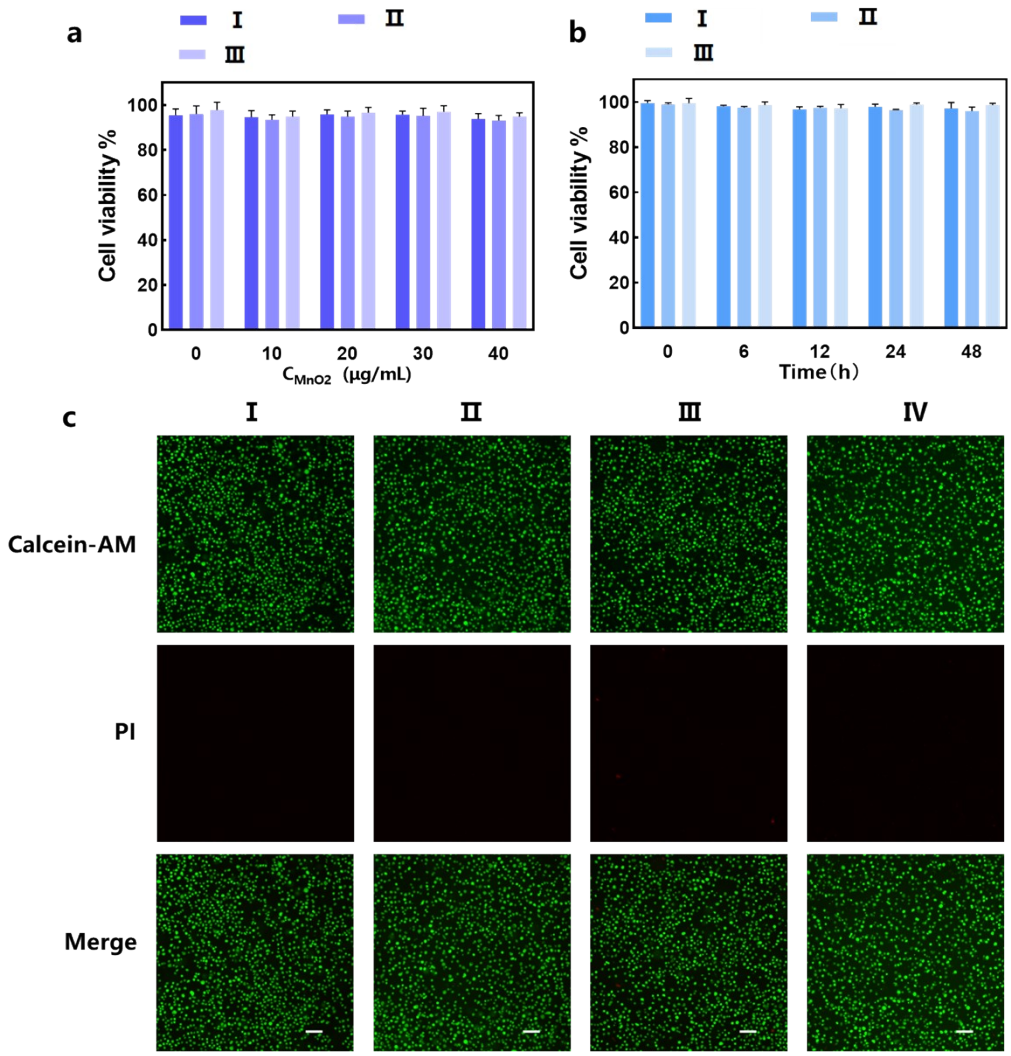


**Fig. S7**. (a) Cell viability of MCF-7 cells treated with different concentrations of $MnO_2$ NS (I), $MnO_2$/Cas12a/crRNA/FQDNA (II), $MnO_2$/Cas12a/crRNA/FQDNA+Lip@substrate/Apt (III) (vs $MnO_2$ NS concentration). (b) Cell viability of MCF-7 cells treated with $MnO_2$NS (I), $MnO_2$/Cas12a/crRNA/FQDNA (II), $MnO_2$/Cas12a/crRNA/FQDNA+Lip@substrate/Apt (III) at different time. (c) Calcein-AM (green, living cells) and PI (red, dead cells) fluorescence images of MCF-7 cells following incubation with different materials. (I：PBS. II：$MnO_2$ NS. III：$MnO_2$/Cas12a/crRNA/FQDNA. IV：$MnO_2$/Cas12a/crRNA/FQDNA+Lip@substrate/Apt) Scale bar: 100 μm.

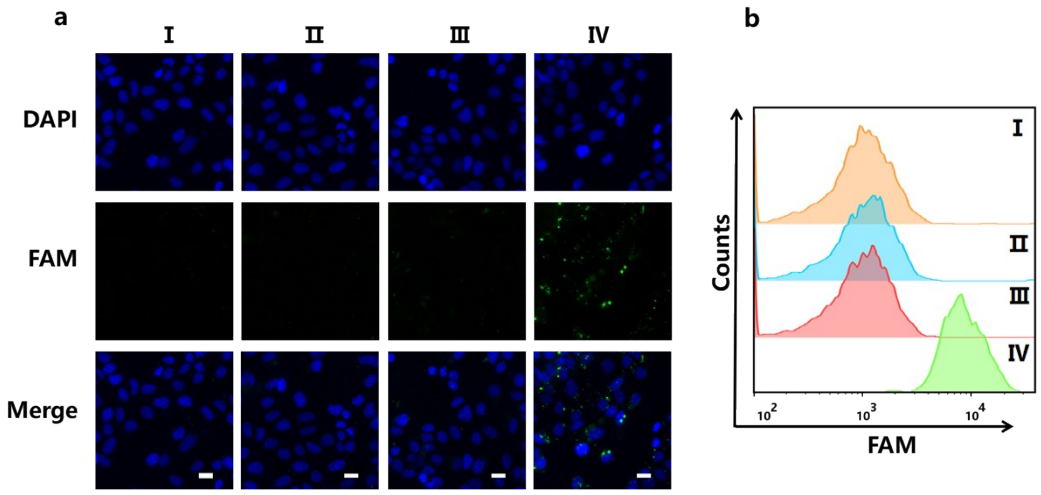


**Fig. S8.** (a) Fluorescence imaging of MCF-7 cells in response to miR-21 under different conditions (I: PBS; II: $MnO_2$/FQDNA; III: $MnO_2$/Cas12a/crRNA/FQDNA; IV: $MnO_2$/Cas12a/crRNA/FQDNA+Lip@substrate/Apt) Scale bar: 20 μm. (b) Flow cytometry of MCF-7 cells vs (a).

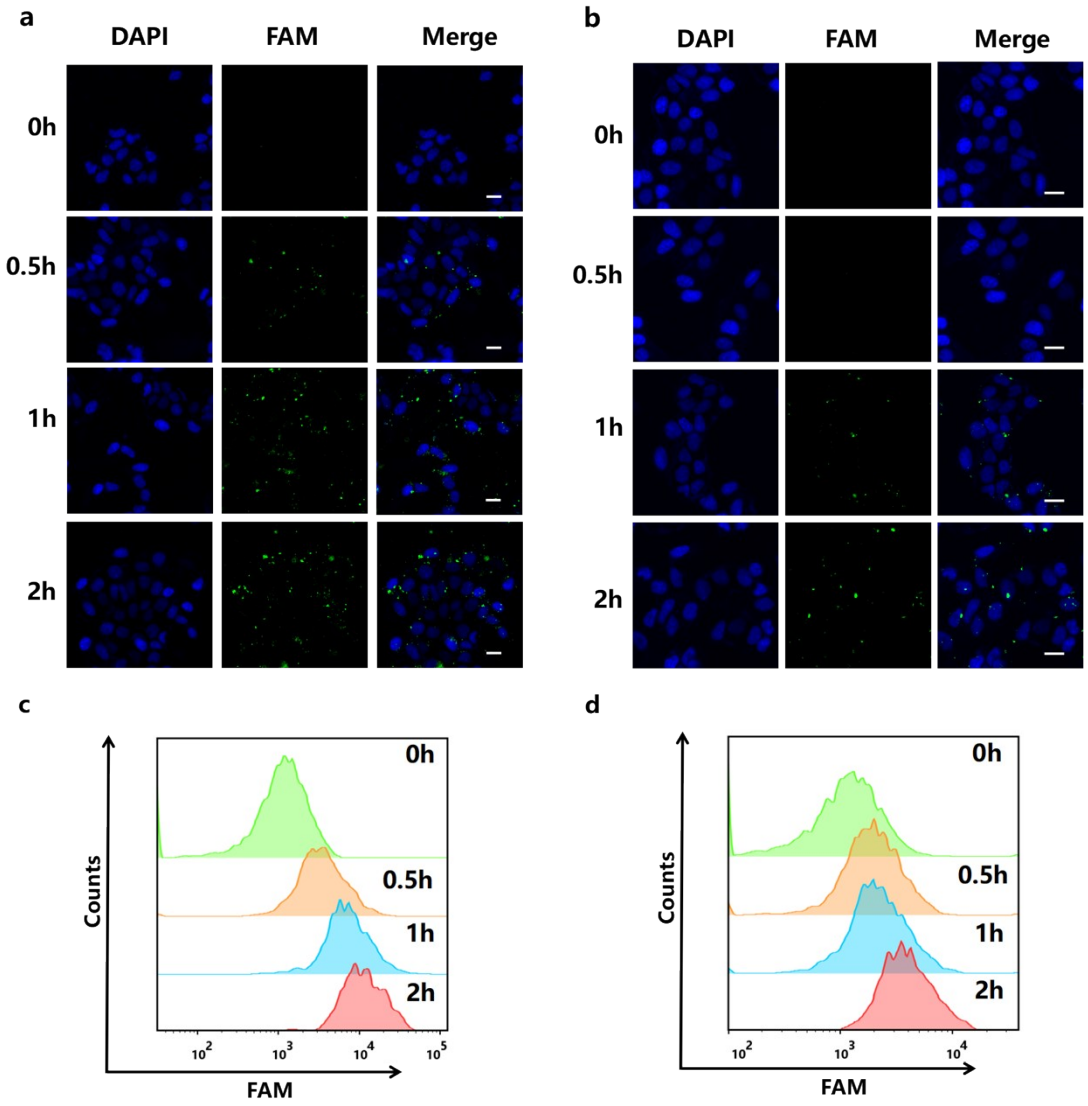


**Fig. S9.** (a-b) Fluorescence pictures after the addition of $MnO_2$/Cas12a/crRNA/FQDNA at different time points by pretreatment for 2 h with (a) Lip@substrate/Apt or (b) Lip@substrate. Scale bar: 20 μm. (c) Flow cytometry of MCF-7 cells vs (a). (d) Flow cytometry of MCF-7 cells vs (b).

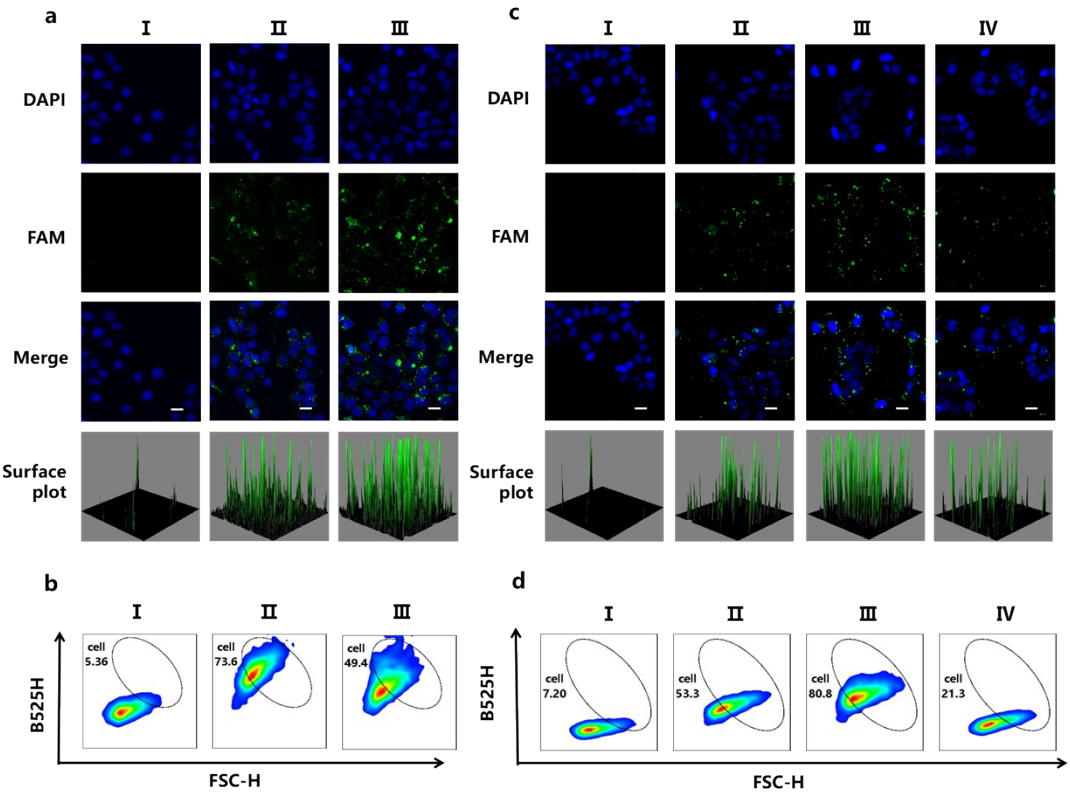


**Fig. S10.** (a) Fluorescence imaging to study the function of GSH (I: cell+PBS; II: cell+$MnO_2$/Cas12a/crRNA/FQDNA+Lip@substrate/Apt; III: cell+NEM+$MnO_2$/Cas12a/crRNA/FQDNA+Lip@substrate/Apt) Scale bar: 20 μm. (b) Flow cytometry of MCF-7 cells vs (a). (c) Fluorescence imaging to study the function of miR-21 (I: cell+PBS; II: cell+$MnO_2$/Cas12a/crRNA/FQDNA+Lip@substrate/Apt; III: cell+Lipofectamine 3000/miR-21+$MnO_2$/Cas12a/crRNA/FQDNA+Lip@substrate/Apt; IV: cell+Lipofectamine 3000/anti-miR-21+$MnO_2$/Cas12a/crRNA/FQDNA+Lip@substrate/Apt) Scale bar: 20 μm. (d) Flow cytometry of MCF-7 cells vs (c).

To verify the dependence of $MnO_2$/Cas12a/crRNA/FQDNA+Lip@substrate/Apt on intracellular GSH, MCF-7 cells were treated with N-ethylmaleimide (NEM) to eliminate endogenous thiols including GSH.[7,8] Compared to the control without NEM treatment, the cells treated with NEM showed very weak fluorescence after incubation with $MnO_2$/Cas12a/crRNA/FQDNA+Lip@substrate/Apt (Fig. S10a), highlighting the GSH dependence of this strategy. Flow cytometry results had shown that, at the same time point, the fluorescence intensity on the FAM channel of NEM-treated cells was weaker compared to the control without NEM treatment, which was consistent with the proposed working mechanism (Fig.

S10b). Since miR-21 expression levels may also change at different stages of tumor development, it was necessary to use $MnO_2$/Cas12a/crRNA/FQDNA+Lip@substrate/Apt to detect changes in miR-21 expression levels. MCF-7 cells were divided into four groups. The first group was treated with PBS. The second group was treated with $MnO_2$/Cas12a/crRNA/FQDNA+ Lip@substrate/Apt. The third group was transfected with Lipofectamine 3000/miR-21+$MnO_2$/Cas12a/ crRNA/FQDNA+Lip@substrate/Apt to increase miR-21 content. The fourth group was transfected with Lipofectamine 3000/anti-miR-21+$MnO_2$/Cas12a/crRNA/FQDNA+Lip@ substrate/Apt to decrease miR-21 content. As shown in Fig. S10c, brighter green fluorescence was observed in the miR-21-transfected group compared to the group of cell+ $MnO_2$/Cas12a/crRNA/FQDNA+Lip@substrate/Apt, while the anti-miR-21-transfected group exhibited much weaker fluorescence. Flow cytometry was used for the same treatment, and it was found that the fluorescence intensity on the FAM channel was consistent with the fluorescence microscopy imaging results (Fig. S10d). These results indicated that $MnO_2$/Cas12a/crRNA/FQDNA+Lip@substrate/Apt could be accurately affected by the different expression levels of miR-21 and displayed different fluorescence intensities.

**Table S1** Oligonucleotides sequences

| Name | Sequence （5’-3’） |
|---|---|
| crRNA[3] | UAAUUUCUACUAAGUGUAGAUACUGAAUCCACAUCAGUCUGAU |
| FQDNA | FAM-TTATT-BHQ1 |
| miR-21 | UAGCUUAUCAGACUGAUGUUGA |
| anti-miR-21[9] | AACAUCAGUCUGAUAAGCUAUU |
| substrate | CATCAACATCAGTCTGATAAGCTAATCAGACTGATGTTGATGAGA CTAAAGACTTTTGTCTTTAGTCT |
| miR-10b | CCCUGUAGAACCGAAUUUGUGU |
| miR-141 | UAACACUGUCUGGUAAAGAUGG |
| miR-let-7f | UGAGGUAGUAGUAGAUUGUAUAGUU |
| miR-210 | CUGUGCGUGUGACAGCGGCUGA |
| miR-let-7a | UGAGGUAGUAGGUUGUAUAGUU |
| MUC1 aptamer[10] | cholesterol-GCAGTTGATCCTTTGGATACCCTGG |

**Notes and references**

1 Zhao, H. Fan, G. Zhou, H. Bai, H. Liang, R. Wang, X. Zhang, W. Tan, *J. Am. Chem. Soc.* 2014, **136**, 11220-11223.

2 W. Wholey, J. Mueller, C. Tan, J. Brooks, J. Zikherman, W. Cheng, *Bioconjug. Chem.* 2020, **31**, 685-697.

3 Q. Chao, Y. Zhang, Q. Li, L. Jiao, X. Sun, X. Chen, L. Zhu, Q. Yang, C. Shang, R. Kong, G. Fan, Z. Song, X. Luo, *Anal. Chem.* 2023, **95**, 15725-15735.

4 H. Hu, S. Guo, Y. Li, K. Dong, Y. Lu, K. Ye, L. Li, X. Zhou, L. Cheng, X. Xiao, *Nat commun.* 2025, **16**, 5035.

5 A. Yuan, R. Sha, W. Xie, G. Qu, H. Zhang, H. Wang, X. Le, G. Jiang, H. Peng, *J. Am. Chem. Soc.* 2024, **146**, 26657–26666

6 Q. Li, Y. Cui, Z. Dai, Z. Yao, M. Li, Q. Cai, D. Kong, *Anal. Chem.* 2025, **97**, 4194–4201

7 X. Hu, Q. Cai, J. Gao, R. Field, G. Chen, N. Jia, Y. Zang, J. Li, X. He, *ACS Appl. Mater. Interfaces* 2024, **16**, 51776-51777.

8 X. Zheng, Z. Yang, Q. Gu, F. Xia, Y. Fu, P. Liu, X. Yin, M. Li, *Autophagy* 2020, **16**, 1838-1850.

9 F. Tang, T. Yang, Z. Zhang, X. Li, Q. Zhong, T. Zhao, L. Gong, *Exp Cell Res*, 2017. 359, 374-383.

10 D. Kalinowska, J. Grabowska, M. Liwinska, *Biosens. Bioelectron* 2019, **126**, 214-221.